Polymer Chemistry

ROYAL SOCIETY OF CHEMISTRY

PAPER

View Article Online
View Journal | View Issue

Cite this: *Polym. Chem.*, 2024, **15**, 1367

Synthesis of stereoregular polymyrcenes using neodymium-, iron- and copper-based catalysts†

Giovanni Ricci, *[a] Antonella Caterina Boccia, [a] Benedetta Palucci, [a] Anna Sommazzi,[b] Francesco Masi,[c] Miriam Scoti, [d] Fabio De Stefano [d] and Claudio De Rosa [d]

Received 28th November 2023,
Accepted 17th February 2024

DOI: 10.1039/d3py01309j

rsc.li/polymers

β-Myrcene was polymerized with catalysts based on pyridyl-imino complexes of neodymium, iron and copper. Highly stereoregular polymers were obtained: in particular, the neodymium-based catalyst gave highly *cis*-1,4 polymers (≥97%), while iron and copper catalysts gave a quite unusual structure in the field of stereospecific polymerization, that is, a predominantly alternating *cis*-1,4-*alt*-3,4 polymer containing *cis*-1,4 unit (five units) sequences within the polymer chain. Structural, thermal and mechanical characterization of the obtained polymers was carried out.

1. Introduction

In the last few decades, interest in renewable resource polymers has grown enormously within both the scientific and industrial communities, and this is essentially attributable to the fact that (i) fossil resources have finite availability and within the next century, they will be nearly depleted; (ii) the main oil-producing countries are generally characterized by political instability, which also leads to a considerable fluctuation in prices with an overall tendency to rise and (iii) the industrial activities associated with their transformation into commodity chemicals and polymers often cause significant environmental problems (*e.g.*, accumulation of CO_2 in the atmosphere, global warming and dangerous climate change). With regard to the greater sustainability of industrial processes, the search for catalytic polymerization systems based on metals with a lower environmental impact and less toxicity than those currently used (*e.g.*, Cr, Co, Ni) is also arousing considerable interest, as indicated, for instance, by the extensive scientific and patent literature on iron-based systems.

In this context, on the basis of the experience previously acquired in the field of the polymerization of conjugated dienes with iron-,[1–4] copper-[5,6] and neodymium-based catalytic systems,[3,7] we have now examined the polymerization of β-myrcene with catalysts based on pyridyl-imino complexes of neodymium, iron and copper.

β-Myrcene is a member of the large family of terpenes, which, due to its structural similarity to isoprene (I) and butadiene (B) and large availability, has recently attracted growing attention as a building block for the synthesis of a vast range of polymers, including the elastomer synthesis: polymers having *cis*-1,4, *trans*-1,4 and 3,4 structures have already been obtained and characterized (Fig. 1).[8–25]

Highly stereoregular poly(myrcene)s, exhibiting somewhat unusual structures as regards the field of conjugated diene polymerization, were obtained, and their synthesis and characterization are reported in the present paper.

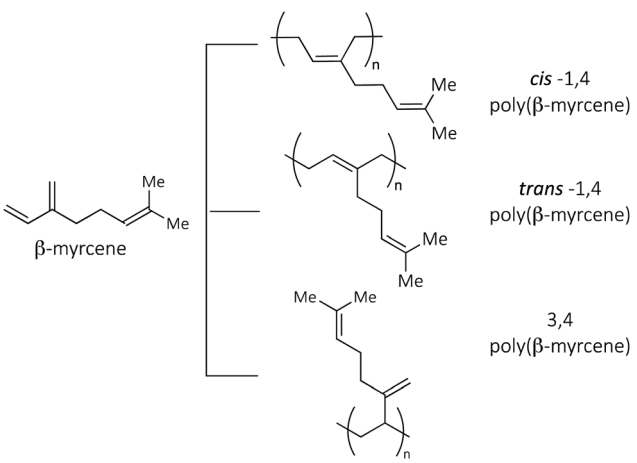

Fig. 1 Stereoregular poly(β-myrcene)s.

[a]*CNR-Istituto di Scienze e Tecnologie Chimiche "Giulio Natta" (SCITEC), via A. Corti 12, I-20133 Milano, Italy. E-mail: giovanni.ricci@scitec.cnr.it*
[b]*Scientific Advisor, Viale Giovanni XXIII 34, I-28100 Novara, NO, Italy*
[c]*Scientific Advisor, Via Galvani 7, I-26866 Sant'Angelo Lodigiano, LO, Italy*
[d]*Dipartimento di Scienze Chimiche, Università di Napoli Federico II, Complesso Monte S.Angelo, Via Cintia, I-80126 Napoli, Italy*

† Electronic supplementary information (ESI) available. See DOI: https://doi.org/10.1039/d3py01309j

2. Experimental

2.1. General procedures and materials

Unless otherwise stated, manipulations of air- and/or moisture-sensitive materials were carried out under an inert atmosphere using a dual vacuum/nitrogen line and standard Schlenk-line techniques. Nitrogen was purified by passage over columns of $CaCl_2$, molecular sieves and BTS catalysts or by passage over the columns Alphagaz Purifiers O_2-Free and H_2O-Free (Air Liquide). Heptane (Merck, 99% pure) and toluene (Aldrich, >99.5%) were refluxed over Na for 8 h and then distilled and stored over molecular sieves. β-Myrcene (Merck, ≥90% pure) was refluxed over CaH_2 for 3 h, then distilled trap-to-trap and stored under dry nitrogen. Iron,[4] copper[6] and neodymium[3,7] complexes were prepared as already reported in the literature. Methylaluminoxane (MAO) (Aldrich, 10 wt% solution in toluene), tetraisobutylaluminoxane (TIBAO) (Akzo Nobel, 10 wt% solution in cyclohexane) and tetrachloroethane-d_2 ($C_2D_2Cl_4$) (Aldrich, >99.5% atom D) were used as received.

2.2. Polymerization

A standard procedure is reported. Myrcene was introduced into a 25 mL dried glass reactor, then the solvent (heptane or toluene) was added and the solution so obtained was brought to the desired polymerization temperature. MAO (or TIBAO) and the metal (Nd or Fe or Cu) complex were then added, as toluene (heptane in the case of neodymium) solution, in order. The polymerization was terminated with methanol containing a small amount of hydrochloric acid, and the polymer was coagulated and repeatedly washed with methanol, and then dried *in vacuo* at room temperature to constant weight.

2.3. Polymer characterization

FTIR spectra were acquired using a PerkinElmer Spectrum Two in attenuated total reflectance (ATR) mode in the spectral range of 4000–500 cm^{-1}. ^{13}C and ^{1}H NMR measurements were carried out on a Bruker Avance 400 spectrometer, operating at 400 MHz for ^{1}H and 100.58 MHz for ^{13}C. The spectra were obtained in $C_2D_2Cl_4$ at 103 °C (hexamethyldisiloxane, HMDS, as internal standard). The concentration of polymer solutions was about 10 wt%. ^{13}C conditions: 10 mm probe, 14.50 μs as a 90° pulse, a relaxation delay of 18 s, and an acquisition time of 1.87 s. Proton broadband decoupling was achieved with a 1 D sequence using bi_waltz_16_32 power-gated decoupling. Two-dimensional heteronuclear ^{1}H–^{13}C experiments were recorded on a Bruker DRX 600 MHz spectrometer thermostated at 330 K. The g-HSQC experiment (gradient-heteronuclear single quantum correlation) was performed by applying a coupling constant $^{1}J_{CH}$ = 140 Hz; data matrix 2 K × 512; number of scans: 128; 7.47 μs as a 90° pulse. The g-HMBC experiments (gradient-heteronuclear multiple bond correlation) were performed by applying a delay of 50 ms for the evolution of long-range coupling; data matrix 2 K × 512; number of scans 128; D1 2.00 s. Data were zero filled and weighted with a sine bell function before Fourier transformation. The microstructure of the resultant polymers was determined by ^{1}H and ^{13}C NMR data, according to the literature.[8,13,16,19] The average molecular weight (M_w) and the molecular weight distribution (M_w/M_n) were obtained using a high-temperature Waters GPCV2000 size exclusion chromatography (SEC) system equipped with a refractometer detector. The experimental conditions consisted of three PL Gel Olexis columns, *ortho*-dichlorobenzene as the mobile phase, 0.8 mL min^{-1} flow rate, and 145 °C. The calibration of the SEC system was performed using eighteen narrow M_w/M_n poly(styrene) standards with M_ws ranging from 162 to 5.6 × 10^6 g mol^{-1}. For SEC analysis, about 12 mg of polymer was dissolved in 5 mL of *ortho*-dichlorobenzene with 0.05% of BHT as an antioxidant.

Details of the characterization of the structure by X-ray diffraction and calorimetry and the analysis of the mechanical properties are reported in the ESI.†

3. Results and discussion

3.1. Polymerization of myrcene with Nd-catalysts

Catalysts obtained by combining the neodymium complex **Nd1** (Fig. 2) with tetraisobutylaluminoxane (TIBAO) provided isoprene polymers with a very high *cis*-1,4 content (≥97%) and molecular weight;[3,7] given the similarity between isoprene and myrcene, both of which are isoprenoids, we expected similar results in the case of myrcene, as actually revealed.

Poly(myrcene) with a rather high molecular weight, narrow polydispersion and extremely high *cis*-1,4 content (around

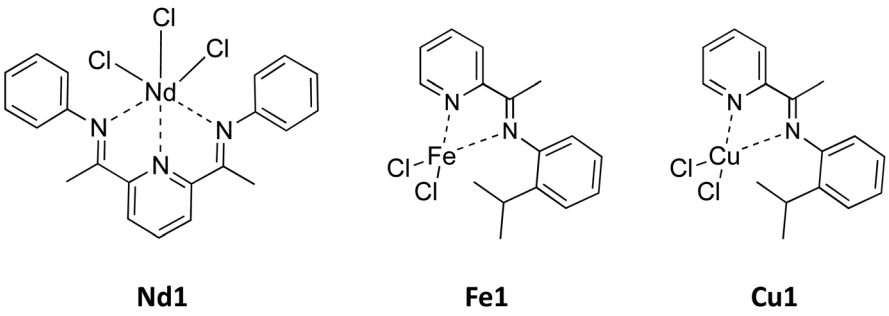

Fig. 2 Neodymium (**Nd1**), iron (**Fe1**) and copper (**Cu1**) complexes used in this work.

97%) was obtained, as shown by their FT-IR (Fig. SI_1†), ^{1}H (Fig. SI_2†) and ^{13}C NMR spectra (Fig. SI_3† and Fig. 4) (Table 1). The glass transition temperature was about −60 °C, quite similar to that of natural rubber. The catalyst activity was rather low, although complete monomer conversions could be achieved.

3.2. Polymerization of myrcene with an Fe-catalyst

The catalytic system **Fe1**/MAO was reported to provide predominantly syndiotactic 1,2 polybutadienes[3,4] and predominantly alternating *cis*-1,4-*alt*-3,4 polyisoprenes containing *cis*-1,4 sequences (three units) within the polymer chain.[3,4] Again, given the similarity between isoprene and myrcene, we expected similar results from the polymerization of myrcene with the same catalysts, and actually poly(myrcene) with a mixed *cis*-1,4/3,4 (68 : 32) structure (Fig. SI_1, SI_2, and SI_3†) was obtained, with the iron system exhibiting extremely high activity (Table 1), much higher with respect to that exhibited by the neodymium system. The polymer molecular weight was around 110 kg × mol^{-1} with a polydispersion of 2, and the glass transition temperature (T_g) was about −57 °C. The distribution mode of the *cis*-1,4 and 3,4 units along the polymeric chain turned out to be quite regular but at the same time rather unusual for the stereospecific polymerization field. The poly(myrcene) obtained with the **Fe1**-based catalyst was in fact characterized by an alternating *cis*-1,4-*alt*-3,4 structure in which, however, long *cis*-1,4 unit sequences (five units) can be detected within the polymer chain (Fig. 3), as suggested by the NMR (^{1}H, ^{13}C and 2D) analysis of the polymer reported below in the Polymer characterization section.

3.3. Polymerization of myrcene with a Cu-catalyst

The **Cu1**/MAO system provided from myrcene a polymer whose ^{13}C NMR spectrum (Fig. S3†) was perfectly superimposable on that of iron poly(myrcene), clearly indicating a perfectly identical polymeric structure, that is, a highly stereoregular alternating *cis*-1,4-*alt*-3,4 structure in which long *cis*-1,4 unit sequences (five units) are present within the polymer chain. The polymer molecular weight was about 262 000 g × mol^{-1} with a polydispersion of 2, and the glass transition temperature (T_g) was about −56 °C. The activity of the copper system resulted to be much lower with respect to that of the iron system, and this could be attributed to the different structures of the active centers in the case of iron and copper, as shown below in section 3.7.

Table 1 Polymerization of β-myrcene with neodymium, iron and copper complex-based catalysts[a]

Entry	Mt_complex (μmol)	Al_type	Al/Mt	Time (h)	Yield (g)	Conv. %	*cis*-1,4[b] (%)	3,4[b] (%)	M_w [c] (kg mol^{-1})	M_w/M_n [c]	T_g [d] (°C)
1	**Nd1** (10)	TIBAO	1000	46	1.39	87.9	97	3	319	2.4	−65
2	**Fe1** (10)	MAO	100	1/4	1.17	74.0	68	32	109.6	2.0	−57
3	**Cu1** (20)	MAO	500	48	0.59	37.3	67	33	261.8	2.0	−56

[a] Polymerization conditions: toluene as solvent (heptane in entry 1), total volume 16 mL; myrcene, 2 mL; 22 °C. [b] Percentage of *cis*-1,4, and 3,4 units determined by ^{1}H and ^{13}C NMR. [c] Average molecular weight (M_w, in kg mol^{-1}) and molecular weight distribution (M_w/M_n) by SEC. [d] Glass transition temperature (T_g) by DSC.

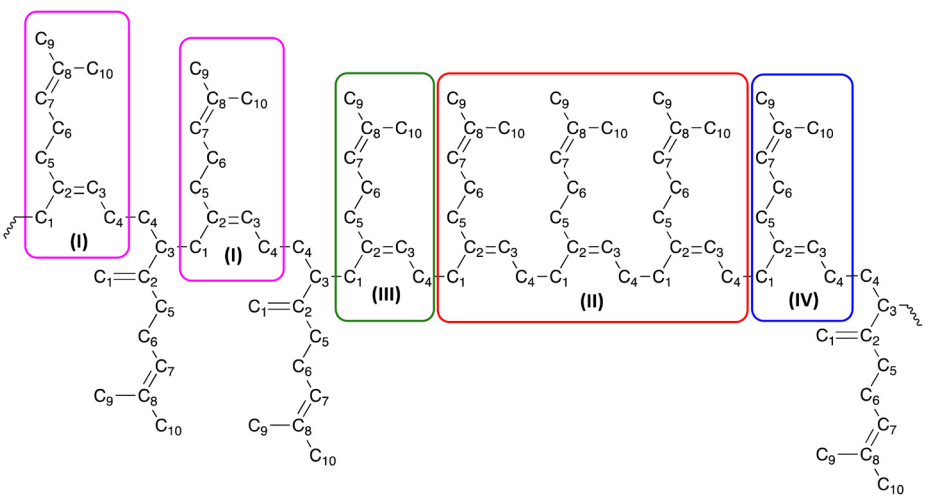

Fig. 3 Predominantly alternating (*cis*-1,4)-*alt*-3,4 poly(myrcene) containing "long" *cis*-1,4 sequences (five units) along the polymer chain, obtained with the **Fe1**/MAO and **Cu1**/MAO systems. The structure shown can be considered as the repeating unit of the polymer chain. Structure (I) represents a *cis* unit involved in an alternating 3,4-(*cis*-1,4)-3,4 sequence; structure (II) represents a *cis* unit involved in a homopolymer (*cis*-1,4)-(*cis*-1,4)-(*cis*-1,4) sequence; structure (III) is a *cis* unit involved in a 3,4-(*cis*-1,4)-(*cis*-1,4) sequence; structure (IV) is a *cis* unit involved in a (*cis*-1,4)-(*cis*-1,4)-3,4 sequence.

3.4. Polymer characterization

The FT-IR spectra of the three different poly(myrcene)s obtained with neodymium-, iron- and copper-based catalysts are shown in Fig. SI_1.† Absorptions at 827 cm^{-1} and 888 cm^{-1} are indicative of the presence of 1,4 and 3,4 units, respectively. The band at 1375 cm^{-1} is indicative of the presence of 1,4 units with a *cis* structure, with the typical absorption of the *trans*-1,4 unit band at 1385 cm^{-1} being not detectable. This means that in poly(myrcene) from Nd almost exclusively *cis*-1,4 units are present, while in poly(myrcene)s from iron and copper both 3,4 and *cis*-1,4 units can be detected. The amount of *cis*-1,4 and 3,4 units was calculated from the ^{1}H NMR spectra (see Fig. SI_2†), according to that reported in the literature.[16,19] The *cis* content of the Nd-poly(myrcene) resulted to be about 97%, while in the Fe- and Cu-poly(myrcene), it was about 70%, with the remaining units being exclusively 3,4. The attribution of the peaks in the case of the neodymium *cis* polymer was carried out on the basis of what has already been reported in the literature, and it is shown in Fig. 4 (C9, 15.72 ppm; C10, 23.56 ppm; C4, 25.00 ppm; C5, 25.35 ppm; C6, 29.01 ppm; C1, 35.11 ppm; C7, 122.90 ppm; C3, 123.05 ppm; C8, 128.99 ppm; and C2, 137.28 ppm). The attribution of the peaks was instead clearly more complicated in the case of poly(myrcene)s from iron- and copper-based catalysts (Fig. 4; peaks corresponding to the C9 carbons and C1 of the 3,4 units are not shown, just to make all the other peaks clearer and more visible. The complete spectra are however reported in ESI Fig. SI_4†), even if the presence of extremely sharp peaks and their distribution immediately directed us towards a rather regular structure, very similar to those found in the case of the poly(isoprene)s previously synthesized by us with the same iron and copper catalytic systems. We therefore hypothesized an alternating *cis*-1,4-*alt*-3,4 structure containing long *cis*-1,4 unit sequences within the polymeric chain (five units, with the *cis*/3,4 molar ratio of about 70/30) (Fig. 3) and then checked this hypothesis through an accurate NMR analysis (^{13}C and two-dimensional experiments).

The polymer microstructure was deeply investigated through two-dimensional ^{1}H–^{13}C HMBC experiments, (heteronuclear multiple bond correlation in Fig. SI_5†) and crucial were the long-term correlations among protons and carbons. In detail, carbon atoms from C7 to C10 have the same chemical shifts for both 3,4- and *cis*-1,4 myrcene units, independent of the comonomer sequences (see Fig. 4). They were assigned starting from the ^{1}H–^{13}C long-term correlations of methyl groups shown in Fig. SI_5,† as follows: C9 at 15.70 ppm; C10 at 23.54 ppm; C7 at 122.88–122.92 ppm; C8 at 128.98–129.17 ppm. Assignment of the 3,4 unit carbons was done in the same way, but starting from the correlations of the olefinic H1 protons at 4.67 ppm (Fig. 5 and Fig. SI_6†), which are as follows: C1 at 107.05 ppm; C2 at 150.72 ppm; C3 at 42.96 ppm; C5 at 32.15 ppm. It is evident that only one signal was observed for each of the two olefin carbons of a myrcene unit having a 3,4 structure, indicating that the 3,4 unit experiences only one type of environment. Finally, to complete the assignment of the 3,4 myrcene unit, C4 was positioned at 34.28 ppm and C6 at 26.5–26.30 ppm.

Apart from this first quite easy assignment, the remaining carbon atoms were assigned step by step due to the complex pattern of almost superimposed signals from Fig. SI_5.† C3 of a *cis*-1,4 unit (**I**) involved in an alternating 3,4-(*cis*-1,4)-3,4 sequence was assigned at 124.40 ppm; C3 of a *cis* 1,4 unit (**IV**) at 124.48 ppm; C3 (**III**) at 124.1 and C3 (**II**) at 123.3 ppm. The differentiation among the olefinic CH atoms (C3 and all the C7 in the spectral region between 122 and 125 ppm) was made considering the absence of correlations in Fig. SI_6† between C3 and the protons of the methyl groups (C9 and C10). Moving on to the assignment of the *cis*-1,4 units, C2 (**I**) was assigned at 135.91 ppm, C2 (**III**) at 136.16 ppm, C2 (**IV**) at 137.38 ppm and C2 (**II**) at 137.59 ppm, while the C5 of all units was positioned between 25.46 and 25.38 ppm. The C1 of *cis*-1,4 units (**II**) was assigned at 35.04 ppm; C1 (**IV**) at 35.21 ppm, and C1 (**I**) and (**III**) at 35.26 ppm. Once the chemical shift of C1 and its protons was known, the (*cis*-1,4)-3,4 sequence was verified by observing the presence of a correlation among the H1 protons of the *cis*-1,4 unit (at 1.86 ppm) with the C2 of the 3,4-unit at 150.72 ppm and with the C3 at 42.96 ppm (Fig. SI_5†). After all, for the assignment of comonomer sequences, the proton spectral region between 4.9 and 5.1 ppm in the HMBC spectrum (Fig. 5) played a crucial role, even if it was very hard to solve considering that at 0.15 ppm, four protons can be found (H7 for both 3,4- and 1,4-myrcene units and H3 for the 1,4-myrcene units involved in (**I**), (**II**), (**III**), and (**IV**) sequences, correlating with more than 12 carbons in the F1 dimension).

3.5 Structural and thermal characterization

The X-ray diffraction profiles of the as-prepared samples of poly(myrcene)s, listed in Table 1, prepared with **Nd1**, **Fe1** and **Cu1** catalysts are reported in Fig. 6A. All three samples show diffuse scattering with two broad maxima at 2θ = 7° and 18°, indicating that the samples are amorphous, although the NMR characterization seems to suggest a remarkable stereoregularity of the polymers. The lack of crystallinity is likely to be attributed to the presence of rather long pendants/side chains (Fig. 3), preventing crystallization in some way. In fact, either the sample with an essentially *cis*-1,4 structure prepared with **Nd1**, or the samples with prevalent alternating *cis*-1,4-*alt*-3,4 structures and long sequences of *cis*-1,4 units prepared with **Fe1** and **Cu1**, present long pendant chains even in the regular *cis*-1,4 units that prevent crystallization. The diffraction profiles of the compression-molded samples prepared by heating the as-polymerized samples at a temperature of 120 °C under a press at low pressure and successive slow cooling to room temperature are shown in Fig. 6B. All samples still show diffuse scattering, indicating that no crystallization occurs upon slow cooling after annealing at high temperature.

The DSC curves of the amorphous as-prepared samples of poly(myrcene)s recorded during heating of the as-prepared samples up to 120 °C, cooling down to −100 °C and successive second heating are shown in Fig. 7. All curves show only a glass transition temperature at low temperature (lower than

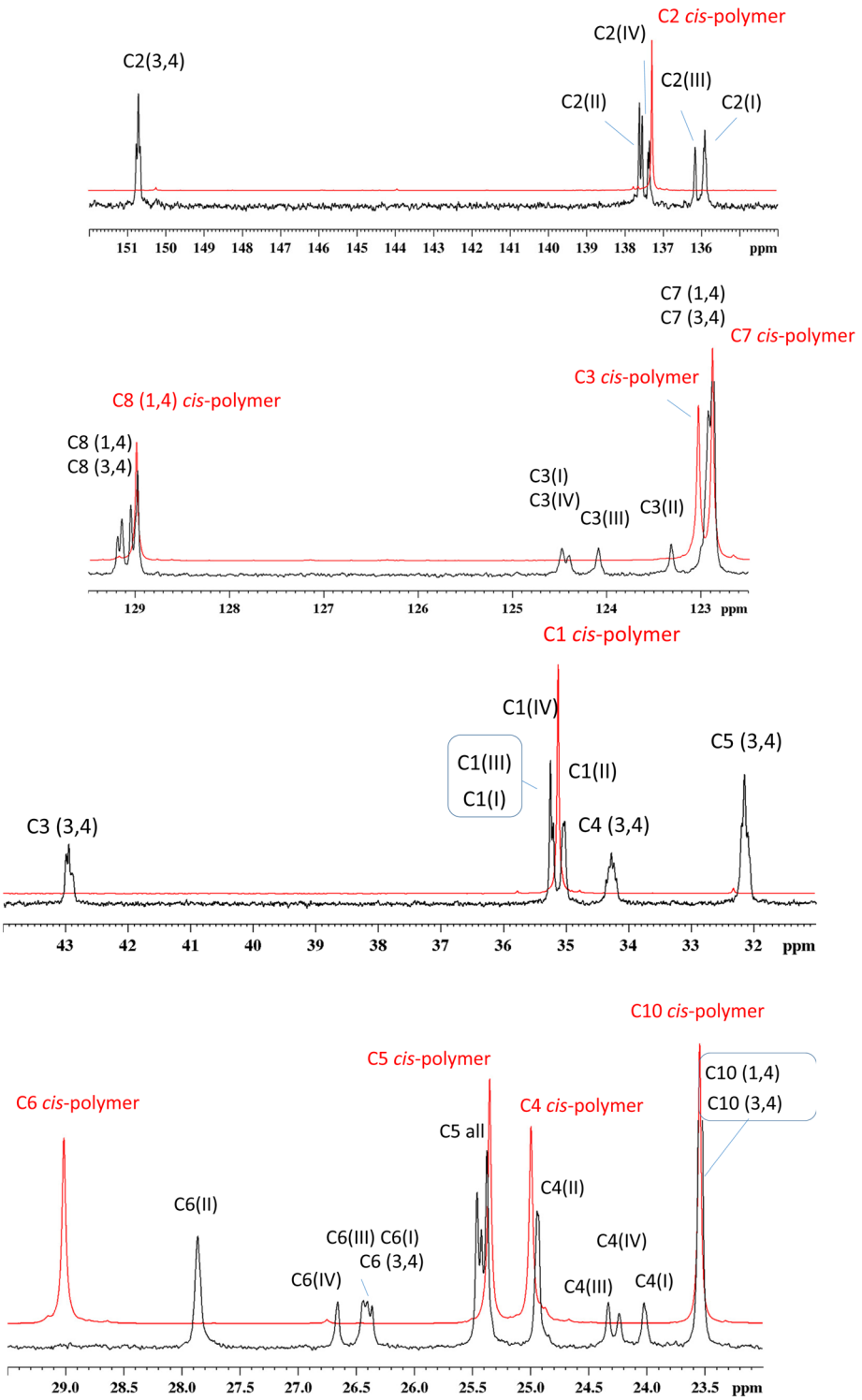

Fig. 4 Assignment of the peaks in the ^{13}C NMR spectra of Nd-polymyrcenes (in red) and Fe-polymyrcenes (in black).

−50 °C) and the absence of any endothermic or exothermic signals. The exact values of the glass transition temperature have been evaluated in the DSC cooling and successive heating curves recorded at the same scanning rates to avoid hysteresis phenomena (Fig. 7 and Table 1). The value of glass transition temperature depends on the molecular structure and, in particular, on the concentration of *cis*-1,4 units, and decreases with increasing concentrations of *cis*-1,4 units. Samples of entries 2 and 3 with 67–68% of *cis*-1,4 units and characterized by prevalent alternating *cis*-1,4/3,4 structures, prepared with iron- and copper-based catalysts, show a glass transition temperature of −56/−57 °C, while the sample of entry 1 with 97% of

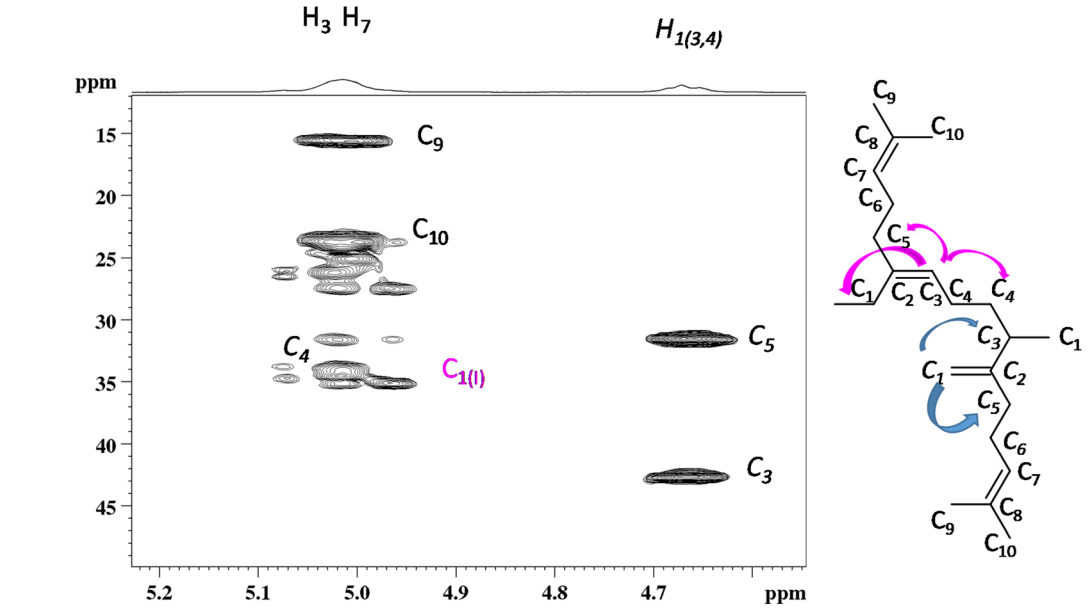

Fig. 5 Expanded spectral region of $^{1}H-^{13}C$ HMBC of poly(myrcene) obtained with the Fe-based catalyst, @600 MHz and 330 K, evidencing peculiar correlations.

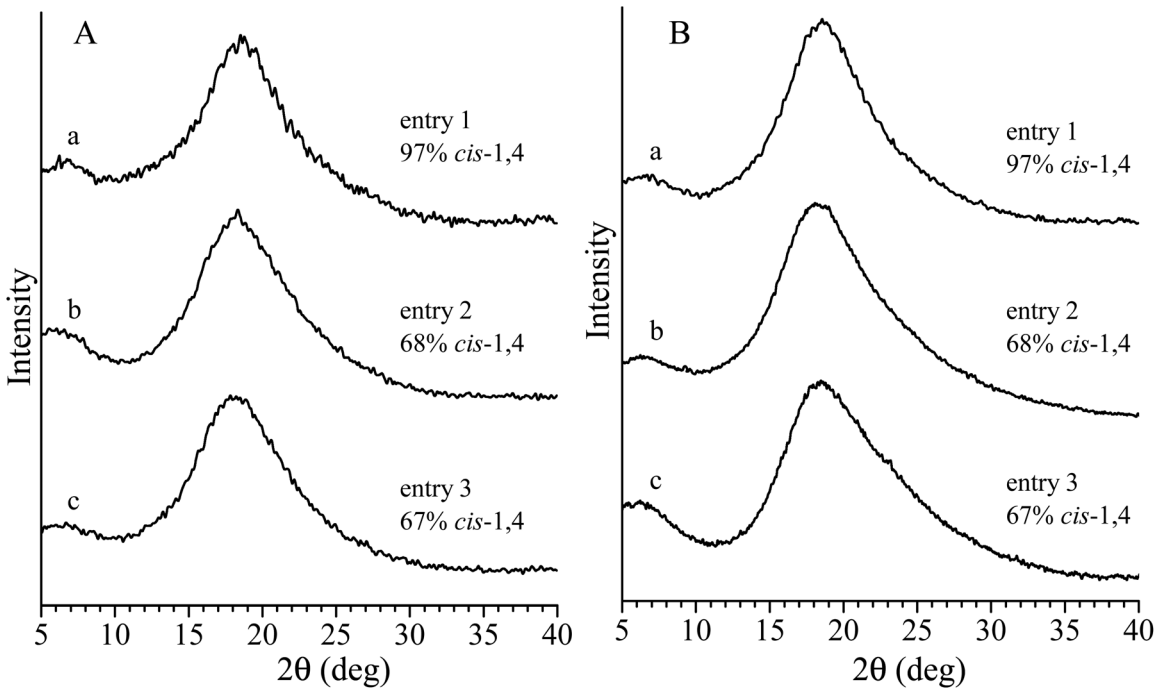

Fig. 6 X-ray powder diffraction profiles of the as-prepared (A) and compression-molded (B) samples of poly(myrcene)s of entry 1 (a), entry 2 (b) and entry 3 (c) of Table 1 prepared with the catalysts **Nd1**, **Fe1** and **Cu1**, respectively.

cis-1,4 units prepared with a neodymium-based catalyst shows the lowest glass transition temperature of about −65 °C.

3.6 Mechanical properties

Compression molded films of poly(myrcene) samples, as listed in Table 1, have been prepared by heating the as-prepared powder samples up to 120 °C under a press at low pressure and slowly cooling down to room temperature. The stress–strain curves of compression-molded films of the three samples of poly(myrcene)s prepared with the three catalysts **Nd1**, **Fe1** and **Cu1** are reported in Fig. 8. All samples show mechanical behavior typical of amorphous polymers with low

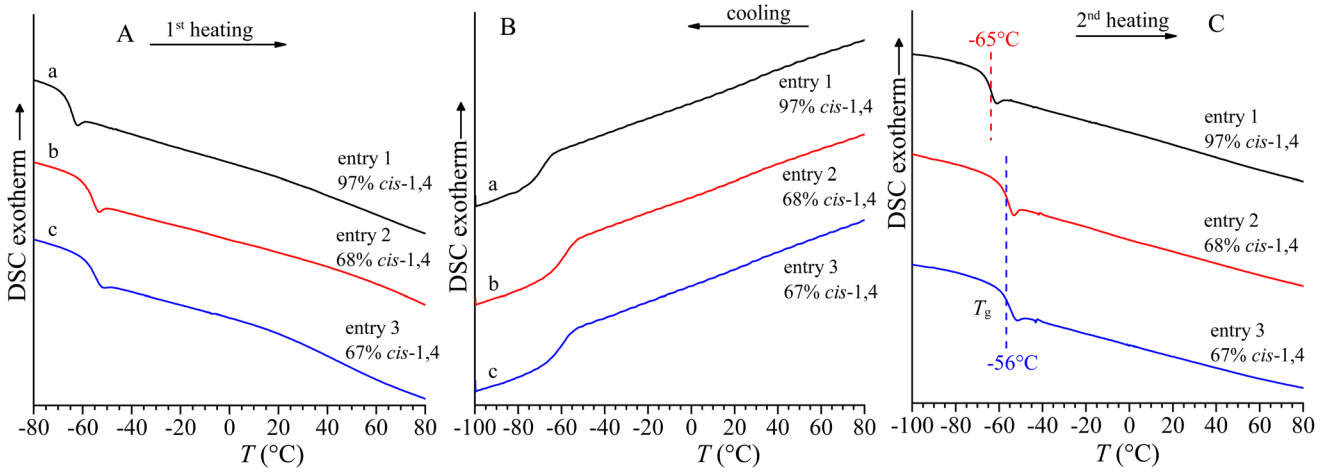

Fig. 7 DSC curves recorded during heating of the as-prepared samples (A), cooling (B) and successive heating (C) at 10 °C min^{-1} scanning rate of samples of poly(myrcene)s of entry 1 (a), entry 2 (b) and entry 3 (c) prepared with the catalysts **Nd1**, **Fe1** and **Cu1**, respectively.

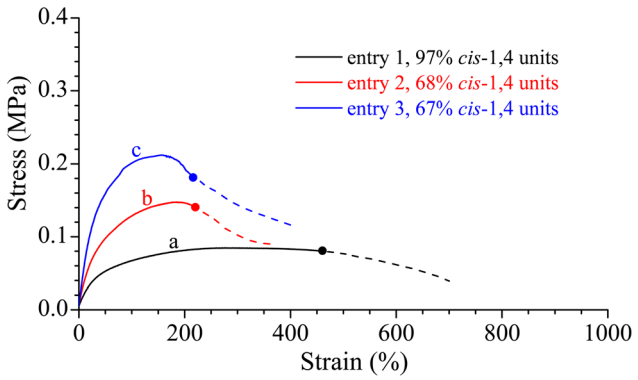

Fig. 8 Stress–strain curves of compression molded films of samples of poly(myrcene)s of entry 1 (a), entry 2 (b) and entry 3 (c) of Table 1, prepared with the catalysts **Nd1**, **Fe1** and **Cu1**, respectively.

modulus and stress values at any strain. Moreover, the samples show uniform deformation without evident yielding up to achieve maximum values of stress at deformations in the range 200–400%. At higher deformations, the samples experience viscous flow without breaking up to 600–800% strain (Fig. 8). In particular, the sample with an almost regular *cis*-1,4 structure (97% of *cis*-1,4 units) and the lowest glass transition temperature, prepared with the neodymium catalyst, shows lower modulus, stress and tensile stress values with remarkably higher ductility. This is due to the almost complete conformational freedom of the single bonds adjacent to the double bonds that results in higher flexibility and easier deformability and a lower modulus and stress, compared to microstructures with high concentrations of 3,4 units. The values of the mechanical parameters are reported in Table 2.

3.7. Some mechanistic considerations

The particular and somewhat unusual structure of the poly(myrcene)s described in the present paper and the different behaviors exhibited by the Nd-, Fe-, and Cu-based catalysts towards butadiene, isoprene, and myrcene lead us to formulate the following remarks:

(a) **Fe1**/MAO and **Cu1**/MAO give (i) essentially alternating *cis*-1,4-*alt*-3,4 polymers, in which, however, long *cis*-1,4 sequences (5 units) are present within the polymer chain, from myrcene; (ii) essentially alternating *cis*-1,4-*alt*-3,4 polymers, in which, however, short *cis*-1,4 sequences (3 units) are present within the polymer chain, from isoprene;[3,4] (iii) predominantly syndiotactic 1,2 polymers from butadiene,[3,4] with some *cis*-1,4 units randomly distributed along the polymer chain. This experimental evidence confirms once more the importance of the monomer structure, and also indeed of the last units of the growing chain, in determining the polymerization selectivity.[2,3,26]

Table 2 Composition, molecular mass (M_w), polydispersion (M_w/M_n), glass transition temperature (T_g), average values of Young's modulus (E), deformation at break (ε_b), stress at break (σ_b) and maximum stress before viscous flow ($\sigma_{b(max)}$) evaluated from the stress–strain curves of Fig. 8 of the compression-molded films of poly(myrcene)s obtained with catalysts **Nd1**, **Fe1** and **Cu1**

Entry	Mt	*cis*-1,4 (%)	3,4 (%)	M_w (kg mol^{-1})	M_w/M_n	T_g [a] (°C)	E (MPa)	ε_b (%)	σ_b (MPa)	$\sigma_{b(max)}$ (MPa)
1	Nd	97	3	319	2.4	−65	0.21 ± 0.02	700 ± 150	0.02 ± 0.01	0.08 ± 0.03
2	Fe	68	32	109.6	2.0	−57	0.42 ± 0.04	361 ± 97	0.09 ± 0.03	0.15 ± 0.02
3	Cu	67	33	261.8	2.0	−56	0.62 ± 0.01	240 ± 70	0.12 ± 0.03	0.21 ± 0.02

[a] Glass transition temperature evaluated from the DSC heating curves of Fig. 7C recorded at a heating rate of 10 °C min^{-1}.

(b) What is stated above, however, is not always true, since **Nd1**/TIBAO invariably supplies high *cis* polymers from butadiene, isoprene and myrcene. This means that the polymer microstructure is always the result of the combination of two main factors, namely the catalytic structure and the monomer structure; sometimes one of the two factors may clearly prevail, making the influence of the other factor practically negligible. In the case of the polymerization of myrcene with the Nd-catalyst, the polymerization mechanism is likely the classical one already reported for other dienes (Fig. 9), with the monomer *cis*-η^4 coordinated to the Nd atom, the growing chain bonded to the Nd-atom through an *anti*-η^3-allyl bond and the insertion of the incoming monomer onto the C3 of the *anti* η^3-allyl unit giving rise to a *cis*-1,4 unit.

(c) We have said above that a rather unusual polymer structure was obtained from β-myrcene with the iron- and copper-based catalysts. In our previous paper,[4] we reported on the polymerization of isoprene with the same iron-based catalyst to give a polymer having a similar structure, that is, an essentially alternating *cis*-1,4-*alt*-3,4 polymer, in which short *cis*-1,4 sequences (3 units) are present within the polymer chain. We had also proposed a possible mechanism for the formation of such an unusual polymer, and we now believe that such a mechanism (Fig. 10) can be re-proposed to account for the formation of a poly(myrcene) having an essentially alternating *cis*-1,4-*alt*-3,4 structure, in which, however, long *cis*-1,4 sequences (5 units) are present within the polymer chain. This scheme of mechanism illustrates, in our opinion, in a plausible way, the subsequent coordination and insertion of myrcene that can lead to the formation of the polymer described in the present paper, even if we realize it does not clarify the reason for the formation of these monomeric sequences (10 units) so regular as to constitute the repeating unit of the polymer itself. In this regard, computational studies could perhaps be of great help.

(d) The catalytic activity of the iron system is much higher than that of the copper system. A plausible explanation for such a difference could be the following: in the case of the iron-based catalyst, the structure of the active center is likely that shown in Fig. 11(a), with the ligand coordinated to the iron atom, the diene *cis*-η^4 coordinated and the growing chain linked to the metal atom through an allyl bond. Such a structure is not possible in the case of the copper-based system, as we would have three electrons in excess of those allowed according to the 18 electron rule.

As already reported in our previous work, we can hypothesize different structures for the catalytic center in the case of the copper catalyst, as shown in Fig. 11(b) and (c).

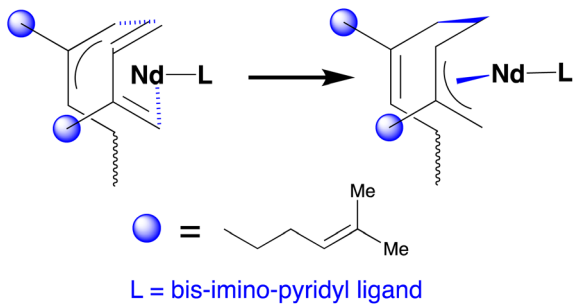

Fig. 9 Scheme of the formation of *cis*-1,4 units in the polymerization of myrcene with the Nd-based catalyst.

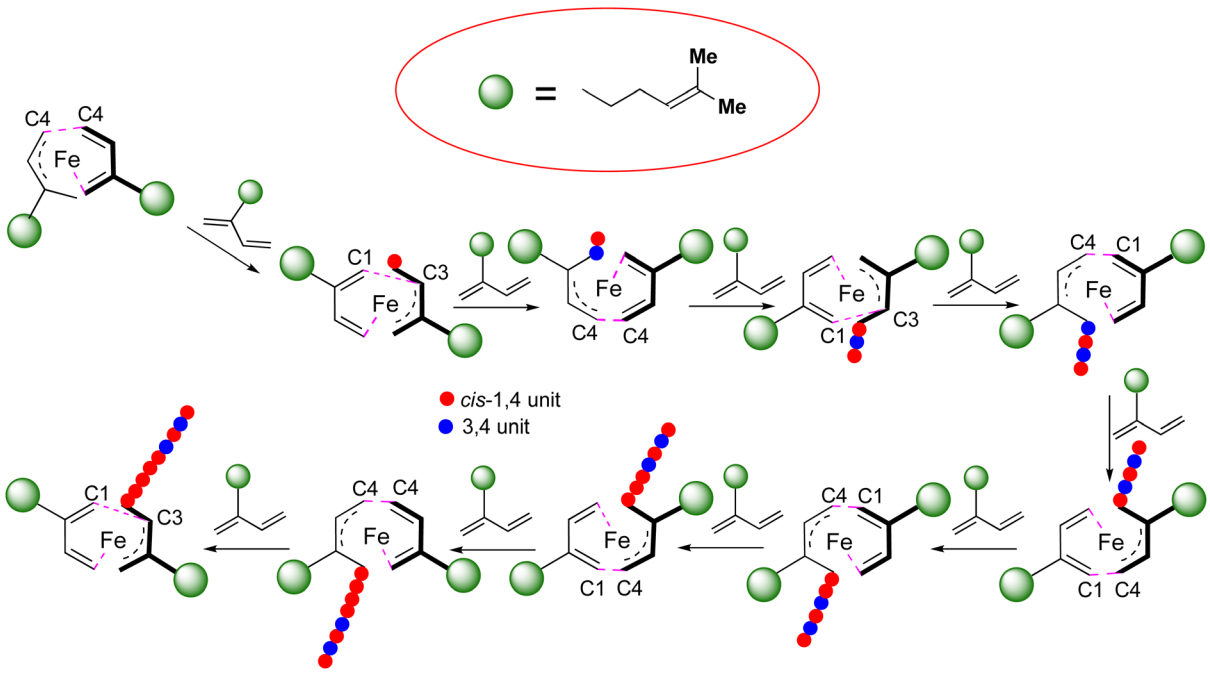

Fig. 10 A possible formation mechanism for the predominantly alternating *cis*-1,4-*alt*-3,4 poly(myrcene) containing long *cis*-1,4 sequences (five units) within the polymer chain.

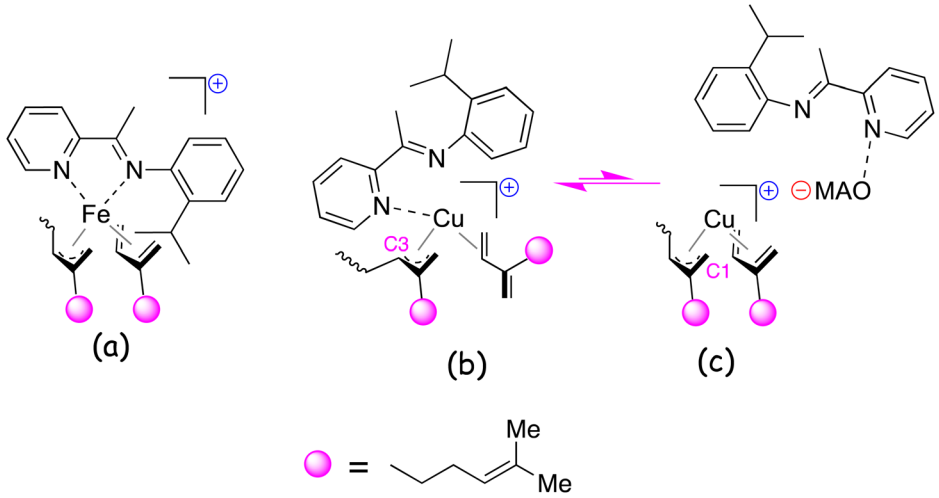

Fig. 11 Possible active site structures.

Myrcene can coordinate *cis*-η^4 with both double bonds, but, in this case, the ligand must have migrated entirely on methylaluminoxane (Fig. 11c), or it can coordinate with only one double bond (*trans*-η^2), and in this case, the ligand can remain coordinated to the copper atom with only one donor atom (Fig. 11b).

A sort of equilibrium can be hypothesized between form (b), with the monomer *trans*-η^2 coordinated and the ligand coordinated with only one nitrogen atom, and form (c), with the monomer *cis*-η^4 coordinated and the ligand onto MAO, with the formation of 1,2 (3,4) units (form (b), through insertion of the incoming monomer to the C3 of the allyl group) rather than *cis*-1,4 (form (c), through insertion of the incoming monomer to the C1 of the allyl group) depending on whether the equilibrium is more shifted towards form (b) or form (c), respectively.

The formation of these active centers with different structures and the oscillation between forms (b) and (c) could be responsible for a lower rate of polymerization, such as to justify the considerable difference in the catalytic activity between iron- and copper-based systems. However, the fact that catalytic centers with different structures (in the case of iron- and copper-based catalysts) can supply the same polymer would seem to indicate that in this case the determining factor of the polymerization stereoselectivity is likely the monomer structure.

4. Conclusion

Highly stereoregular polymers were obtained from myrcene using neodymium, iron and copper organometallic complexes, having a well-defined structure, in combination with methylaluminoxane.

In particular, highly *cis*-1,4 polymers have been obtained with neodymium-based systems, while polymers having a rather unusual structure as regards the stereospecific polymerization of conjugated dienes, that is, a mainly alternating *cis*-1,4-*alt*-3,4 structure, but with regular *cis*-1,4 sequences (5 units) along the polymer chain, were obtained by means of iron and copper catalysts. The polymers have generally high molecular weights and glass transition temperature values of around −60 °C, similar to those of natural rubber, which makes them of potential interest for possible use as elastomers.

The polymers are amorphous, despite the high degree of stereoregularity exhibited, as indicated by NMR analysis. The lack of crystallinity is probably due to the presence of rather long pendants/side chains even in a rather regular molecular structure that prevents crystallization. In fact, either the sample with a prevalent *cis*-1,4 structure prepared with **Nd1** or the samples with prevalent alternating *cis*-1,4-*alt*-3,4 structures and long sequences of *cis*-1,4 units prepared with **Fe1** and **Cu1** present long pendant chains even in the regular *cis*-1,4 units that prevent crystallization.

As a consequence, the samples show the mechanical behavior of soft materials with uniform deformation without evident yielding up to achieve maximum values of stress at deformations in the range 200–400%. At higher deformations, the samples experience viscous flow without breaking up to 600–800% strain.

Finally, the different behaviors exhibited by the **Fe1**/MAO and **Cu1**/MAO systems towards butadiene, isoprene and myrcene represent a further confirmation of the remarkable influence of the monomer structure on the polymerization selectivity.

Data availability

The data that supports the findings of this study are available in the FigShare repository at DOI: **https://doi.org/10.6084/m9.figshare.25259563**.

Conflicts of interest

There are no conflicts of interest to declare.

Acknowledgements

The author B.P. thanks the Horizon Europe research and innovation program for the Postdoctoral Fellowship under the Marie Curie Grant Agreement (POLYFUN, No. 101062863).

References

1 G. Ricci, D. Morganti, A. Sommazzi, R. Santi and F. Masi, Polymerization of 1,3-dienes with iron complexes based catalysts: Influence of the ligand on catalyst activity and stereospecificity, *J. Mol. Catal. A: Chem.*, 2003, **204–205**, 287–293.

2 G. Ricci, A. Sommazzi, F. Masi, M. Ricci, A. Boglia and G. Leone, Well Defined Transition Metal Complexes with Phosphorus and Nitrogen Ligands for 1,3-Dienes Polymerization, *Coord. Chem. Rev.*, 2010, **254**, 661–676.

3 G. Ricci, G. Pampaloni, A. Sommazzi and F. Masi, Dienes Polymerization: where we are and what lies ahead, *Macromolecules*, 2021, **54**, 5879–5914.

4 G. Ricci, G. Leone, G. Zanchin, B. Palucci, A. C. Boccia, A. Sommazzi, F. Masi, S. Zacchini, M. Guelfi and G. Pampaloni, Highly Stereoregular 1,3-Butadiene and Isoprene Polymers through Monoalkyl–N–Aryl Substituted Iminopyridine Iron Complex-Based Catalysts: Synthesis and Characterization, *Macromolecules*, 2021, **54**, 9947–9959.

5 G. Ricci, G. Leone, G. Zanchin, F. Masi, M. Guelfi and G. Pampaloni, Dichloro(2,2′-bipyridine)copper/MAO: An Active and Stereospecific Catalyst for 1,3- Diene Polymerization, *Molecules*, 2023, **28**, 374.

6 G. Ricci, G. Leone, G. Zanchin, F. Masi, S. Zacchini, G. Bresciani, M. Guelfi and G. Pampaloni, Iminopyridine Copper Complex-based Catalysts for 1,3-Dienes Stereospecific Polymerization, *Macromol. Chem. Phys.*, 2023, **224**, 2300037.

7 G. Ricci, A. Sommazzi, G. Leone, A. Boglia, M. Caldararo and F. Masi, Bis-imine pyridine complex of lanthanides, catalytic system comprising said bis-imine pyridine complex and process for the (co)polymerization of conjugated dienes. WO2013037913A1, 2013.

8 R. A. Newmark and R. N. Majumdar, 13C-NMR Spectra of cis- Polymyrcene and cis-Polyfarnesene, *J. Polym. Sci., Part A: Polym. Chem.*, 1988, **26**, 71–77.

9 A. Gandini, Polymers from Renewable Resources: A Challenge for the Future of Macromolecular Materials, *Macromolecules*, 2008, **41**, 9491–9504.

10 A. Behr and L. Johnen, Myrcene as a natural base chemical in sustainable chemistry: a critical review, *ChemSusChem*, 2009, **2**, 1072–1095.

11 A. Gandini, The irruption of polymers from renewable resources on the scene of macromolecular science and technology, *Green Chem.*, 2011, **13**, 1061–1083.

12 J. Zhao and H. Schlaad, Synthesis of Terpene-Based Polymers, *Adv. Polym. Sci.*, 2011, **253**, 151–190.

13 J. Raynaud, J. Y. Wu and T. Ritter, Iron-catalyzed polymerization of isoprene and other 1,3-dienes, *Angew. Chem., Int. Ed.*, 2012, **51**, 11805–11808.

14 S. Loughmari, A. Hafid, A. Bouazza, A. El Bouadili, P. Zinck and M. Visseaux, Highly Stereoselective Coordination Polymerization of β-Myrcene from a Lanthanide-Based Catalyst: Access to Bio- Sourced Elastomers, *J. Polym. Sci., Part A: Polym. Chem.*, 2012, **50**, 2898–2905.

15 P. A. Wilbon, F. Chu and C. Tang, Progress in renewable polymers from natural terpenes, terpenoids, and rosin, *Macromol. Rapid Commun.*, 2013, **34**, 8–37.

16 S. Georges, M. Bria, P. Zinck and M. Visseaux, Polymyrcene microstructure revisited from precise high-field nuclear magnetic resonance analysis, *Polymer*, 2014, **55**, 3869–3878.

17 A. Gandini and T. M. Lacerda, From monomers to polymers from renewable resources: recent advances, *Prog. Polym. Sci.*, 2015, **48**, 1–39.

18 B. Liu, L. Li, G. Sun, D. Liu, S. Li and D. Cui, Isoselective 3,4- (co)polymerization of bio-renewable myrcene using NSN-ligated rare-earth metal precursor: an approach to a new elastomer, *Chem. Commun.*, 2015, **51**, 1039–1041.

19 R. E. Diaz de Leòn Gómez, F. J. Enrìquez-Medrano, H. Maldonado Textle, R. Mendoza Carrizales, K. Reyes Acosta, H. R. Lòpez Gonzàlez, J. L. Olivares Romero and L. E. Lugo Uribe, Synthesis and Characterization of High cis-Polymyrcene using Neodymium-Based Catalysts, *Can. J. Chem. Eng.*, 2016, **94**, 823–832.

20 M. Naddeo, A. Buonerba, E. Luciano, A. Grassi, A. Proto and C. Capacchione, Stereoselective polymerization of biosourced terpenes myrcene and ocimene and their copolymerization with styrene promoted by titanium catalysts, *Polymer*, 2017, **131**, 151–159.

21 M. Winnacker, Pinenes: Abundant and Renewable Building Blocks for a Variety of Sustainable Polymers, *Angew. Chem., Int. Ed.*, 2018, **57**, 14362–14371.

22 W. Li, J. Zhao, X. Zhang and D. Gong, Capability of PN3-type cobalt complexes toward selective co-polymerization of myrcene, butadiene, and isoprene: access to biosourced polymers, *Ind. Eng. Chem. Res.*, 2019, **58**, 2792–2800.

23 X. Jia, W. Li, J. Zhao, F. Yi, Y. Luo and D. Gong, Dual Catalysis of the Selective Polymerization of Biosourced Myrcene and Methyl Methacrylate Promoted by Salicylaldiminato Cobalt(II) Complexes with a Pendant Donor, *Organometallics*, 2019, **38**, 278–288.

24 Q. Gan, Y. Xu, E. W. Huang, W. Luo, Z. Hu, F. Tan, X. Jia and D. Gong, Utilization of bio-sourced myrcene for efficient preparation of highly cis-1,4 regular elastomer via a neodymium catalyzed copolymerization strategy, *Polym. Int.*, 2020, **69**, 763–770.

25 Z. Chen, X. Xu, Y. Zhou, H. Liu, S. Cui and D. Gong, Fe-based catalyst with diphenylphosphite as donor for stereopolymerization of butadiene, isoprene, and myrcene, *J. Appl. Polym. Sci.*, 2022, e53127.

26 L. Porri, A. Giarrusso and G. Ricci, Recent views on the mechanism of diolefin polymerization with transition metal initiator systems, *Prog. Polym. Sci.*, 1991, **16**, 405–441.

